



**HAL**  
open science

## Persistent Draining of the Stratospheric $^{10}\text{Be}$ Reservoir After the Samalas Volcanic Eruption (1257 CE)

Mélanie Baroni, Edouard Bard, Jean-robot Petit, Sophie Viseur

### ► To cite this version:

Mélanie Baroni, Edouard Bard, Jean-robot Petit, Sophie Viseur. Persistent Draining of the Stratospheric  $^{10}\text{Be}$  Reservoir After the Samalas Volcanic Eruption (1257 CE). *Journal of Geophysical Research: Atmospheres*, 2019, 124 (13), pp.7082-7097. 10.1029/2018JD029823 . hal-02293033

**HAL Id: hal-02293033**

**<https://hal.science/hal-02293033>**

Submitted on 13 Aug 2021

**HAL** is a multi-disciplinary open access archive for the deposit and dissemination of scientific research documents, whether they are published or not. The documents may come from teaching and research institutions in France or abroad, or from public or private research centers.

L'archive ouverte pluridisciplinaire **HAL**, est destinée au dépôt et à la diffusion de documents scientifiques de niveau recherche, publiés ou non, émanant des établissements d'enseignement et de recherche français ou étrangers, des laboratoires publics ou privés.

Copyright

# JGR Atmospheres

## RESEARCH ARTICLE

10.1029/2018JD029823

†Georges Aumaitre, Didier L. Bourlès, Karim Keddadouche

## Persistent Draining of the Stratospheric $^{10}\text{Be}$ Reservoir After the Samalas Volcanic Eruption (1257 CE)

Mélanie Baroni<sup>1</sup> , Edouard Bard<sup>1</sup> , Jean-Robert Petit<sup>2</sup>, Sophie Viseur<sup>1</sup> , and ASTER Team<sup>1,†</sup>

<sup>1</sup>Aix Marseille University, CNRS, IRD, INRA, Coll France, CEREGE, Aix-en-Provence, France, <sup>2</sup>IGE, Université Grenoble Alpes, CNRS, IRD, Grenoble INP, Grenoble, France

### Key Points:

- Beryllium-10 deposition on polar ice sheets is influenced by stratospheric volcanic eruptions
- The biggest volcanic eruption of the last millennium, the Samalas (1257 CE), probably drained out the polar stratospheric  $^{10}\text{Be}$  reservoir over a decade
- Solar reconstructions based on  $^{10}\text{Be}$  ice core records must take into account volcanic disturbance

### Supporting Information:

- Supporting Information S1
- Data Set S1

### Correspondence to:

M. Baroni,  
baroni@cerege.fr

### Citation:

Baroni, M., Bard, E., Petit, J.-R., Viseur, S., & ASTER Team (2019). Persistent draining of the stratospheric  $^{10}\text{Be}$  reservoir after the Samalas volcanic eruption (1257 CE). *Journal of Geophysical Research: Atmospheres*, 124, 7082–7097. <https://doi.org/10.1029/2018JD029823>

Received 12 OCT 2018

Accepted 15 MAY 2019

Accepted article online 12 JUN 2019

Published online 13 JUL 2019

**Abstract** More than 2,000 analyses of beryllium-10 ( $^{10}\text{Be}$ ) and sulfate concentrations were performed at a nominal subannual resolution on an ice core covering the last millennium as well as on records from three sites in Antarctica (Dome C, South Pole, and Vostok) to better understand the increase in  $^{10}\text{Be}$  deposition during stratospheric volcanic eruptions. A significant increase in  $^{10}\text{Be}$  concentration is observed in 14 of the 26 volcanic events studied. The slope and intercept of the linear regression between  $^{10}\text{Be}$  and sulfate concentrations provide different and complementary information. Slope is an indicator of the efficiency of the draining of  $^{10}\text{Be}$  atoms by volcanic aerosols depending on the amount of  $\text{SO}_2$  released and the altitude it reaches in the stratosphere. Intercept gives an image of the  $^{10}\text{Be}$  production in the stratospheric reservoir, ultimately depending on solar modulation. The Samalas event (1257 CE) stands out from the others as the biggest eruption of the last millennium with the lowest positive slope of all the events. We hypothesize that the persistence of volcanic aerosols in the stratosphere after the Samalas eruption has drained the stratospheric  $^{10}\text{Be}$  reservoir for a decade, meaning that solar reconstructions based on  $^{10}\text{Be}$  should be considered with caution during this period. The slope of the linear regression between  $^{10}\text{Be}$  and sulfate concentrations can also be used to correct the  $^{10}\text{Be}$  snow/ice signal of the volcanic disturbance.

## 1. Introduction

The cosmogenic nuclide of beryllium 10 ( $^{10}\text{Be}$ ) measured in ice cores is an indirect proxy for past solar activity (e.g., Bard et al., 1997; Beer et al., 1990; Berggren et al., 2009; Cauquoin et al., 2014; Delaygue & Bard, 2011; Horiuchi et al., 2008; Raisbeck et al., 1990; Steinhilber et al., 2012; Wu et al., 2018) and for geomagnetic excursions or reversals (e.g., Beer et al., 1988; Finkel & Nishiizumi, 1997; Raisbeck et al., 2017, 2006; Yiou et al., 1997). In the atmosphere it is produced from spallation reactions on oxygen and nitrogen atoms induced by primary cosmic rays, whose flux is modulated by the magnetic fields of the Earth and the Sun.

Unlike the cosmogenic isotope of carbon-14 ( $^{14}\text{C}$ ), which is globally mixed through the gaseous form of carbon dioxide ( $\text{CO}_2$ ),  $^{10}\text{Be}$  atoms attach onto aerosols to fall to the Earth's surface (e.g., Raisbeck et al., 1981). One of the consequences of this peculiarity is the increase in  $^{10}\text{Be}$  deposition, which can be observed in glaciological archives corresponding to periods of stratospheric volcanic eruption (Baroni et al., 2011).

Volcanic eruptions release large amounts of sulfur dioxide ( $\text{SO}_2$ ) which oxidizes over the course of a few months to sulfate (e.g., McCormick et al., 1995), itself a primary chemical component for aerosols formation. The stratospheric burden of sulfate aerosols always exceeds that of  $^{10}\text{Be}$ , even in nonvolcanic conditions (Heikkilä et al., 2013). However, the mechanism behind the increase in  $^{10}\text{Be}$  deposition flux is not linked to the balance between the amount of sulfate and  $^{10}\text{Be}$  but rather to the microphysics of aerosols, that is to say, to their dynamic (Baroni et al., 2011; Delaygue et al., 2015). Aerosol microphysics can be described in four steps: heterogeneous nucleation, condensation of sulfuric acid and water, coagulation, and gravitational sedimentation (e.g., Bekki & Pyle, 1992). Volcanic eruptions generate supplemental sulfate aerosols on a short time scale, accelerating this four-step cycle and, in particular, the gravitational sedimentation because of a higher collision rate making larger aerosols than in nonvolcanic conditions (e.g., Pinto et al., 1989; Timmreck, 2012), and finally impacting  $^{10}\text{Be}$  atoms deposition (Baroni et al., 2011).

Increases in  $^{10}\text{Be}$  concentration observed in measurements obtained in a snow pit at Vostok (Antarctica) correspond to the period of sulfate deposition associated to the stratospheric eruptions of the Agung (1963 CE) and Pinatubo (1991 CE). (Baroni et al., 2011).  $^{10}\text{Be}$  and sulfate concentrations were measured in the

same sample, allowing for their direct comparison. A linear relationship could be inferred, and a correction based on the slope of the line was applied in order to remove the volcanic contribution from the  $^{10}\text{Be}$  record (Baroni et al., 2011) to better isolate the solar component.

There is only one study to date which covers the last 60 years and which was designed for that purpose (Baroni et al., 2011). Other Greenlandic and Antarctic ice core records exhibit  $^{10}\text{Be}$  peaks corresponding to dates of known volcanic eruptions such as Kuwae (1459 CE) or Tambora events (1815 CE) (Bard, 1997; Berggren et al., 2009; Horiuchi et al., 2008), but the interpretation is limited because either (i) the resolution is too low, and/or (ii) the sulfate concentration is not always available and has not been measured from  $^{10}\text{Be}$  samples preventing from direct comparison between both proxies.

Volcanic eruption source parameters (e.g., amount of  $\text{SO}_2$  emitted, plume height, eruption season, and geographic location) all differ, and eruptions may occur at any phase of solar activity. For this reason, we investigate 26 volcanic events recorded over the last millennium, at three sites in Antarctica (Dome C, Vostok, and South Pole) in order to better understand their impact on the  $^{10}\text{Be}$  deposition. Only two of them, Pinatubo (1991 CE) and Agung (1963 CE), benefited from direct observations. Petrological studies exist for some older eruptions such as the Cosiguina event (1835 CE), which may have been comparable to the Pinatubo eruption (Longpré et al., 2014), and the Tambora event (1815 CE) (Self et al., 2004; Sigurdsson & Carey, 1989). However, most volcanic eruptions of the last millennium are little understood and lacking in direct or petrological observations. For these unknown eruptions, we will interpret our  $^{10}\text{Be}$  data using information on the stratospheric/tropospheric nature of the eruptions provided by two independent methods, namely, (i) the bipolar deposition of volcanic sulfate (henceforth bipolar events) and (ii) the sulfur isotopic composition of sulfate.

Bipolar events are interpreted as a result of tropical stratospheric eruptions (Gao et al., 2007; Langway et al., 1995; Sigl et al., 2013, 2015) whose volcanic sulfate aerosols are spread out all over the globe before being deposited in Greenland and Antarctica. However, if two eruptions (tropospheric or stratospheric) occurred in the same year in the middle or high latitudes of each hemisphere, peaks of sulfate will also be recorded in Greenland and Antarctica (Cole-Dai et al., 2009; Yalcin et al., 2006). A reliable method for identifying a stratospheric eruption is the presence of a sulfur isotopic anomaly ( $\Delta^{33}\text{S}$ ) in volcanic sulfate. Due to non-mass-dependent fractionation, this isotopic anomaly appears when sulfured gases such as  $\text{SO}_2$  are exposed to wavelengths lower than 310 nm (Farquhar et al., 2001; Ono et al., 2013; Whitehill et al., 2015), which corresponds to a spectral window available in the stratosphere in today's atmosphere. Several studies have used this peculiarity to identify stratospheric eruptions in ice core records (Baroni et al., 2007, 2008; Cole-Dai et al., 2009, 2013; Gautier et al., 2018, 2019; Lanciki et al., 2012; Savarino, Romero, et al., 2003).

Finally, we focus on the most important volcanic eruption of the last millennium, the Samalas event (1257 CE), which released  $(158 \pm 12)$  Tg of sulfur dioxide ( $\text{SO}_2$ ) to an altitude of 43 km in the stratosphere (Lavigne et al., 2013; Vidal et al., 2016). The discussion will consider the impact of this massive eruption on the  $^{10}\text{Be}$  ice core signal and its implications for solar reconstructions because at annual resolution, a  $^{10}\text{Be}$  peak induced by a volcanic eruption may be confused with a solar particle event, such as those of 775 CE and 993 CE which have been previously detected in ice cores (Mekhaldi et al., 2015; Miyake et al., 2015; Sigl et al., 2015). It also alters the preservation of the 11-year solar cycle (Baroni et al., 2011). The interpretation of  $^{10}\text{Be}$  ice core records in terms of solar activity requires proper identification of volcanic disturbances and a better understanding of the mechanism behind the washout of  $^{10}\text{Be}$  atoms from their stratospheric reservoir located between 10 and 17 km altitude where  $^{10}\text{Be}$  production and  $^{10}\text{Be}$  concentration are the highest, respectively (Delaygue et al., 2015; Kovaltsov & Usoskin, 2010).

## 2. Method

### 2.1. Sites and Samples Description

As part of the French VOLSOL project (Acronym for 'Forçages climatiques naturels volcanique et solaire'), six ice cores of 90–100 m depth were drilled 1 m apart at the Italian-French station of Concordia-Dome C, in Antarctica, in 2010/2011 (75°60'S, 123°21'E; elevation 3,240 m; mean annual temperature  $-54.5$  °C; accumulation 2.5 cm water equivalent/year (we/year); EPICA community members, 2004). Five ice cores were used for the isotopic composition of volcanic sulfate (Gautier et al., 2016, 2018, 2019), and one was

dedicated to the study of cosmogenic isotopes of  $^{10}\text{Be}$  and  $^{36}\text{Cl}$ . The latter is named VOLSOL-6. Both  $^{10}\text{Be}$  and sulfate concentrations were measured in identical samples in the first 54 m of the ice core, cut into 3-cm slices. More than 1,600  $^{10}\text{Be}$  samples were analyzed, allowing to reach a nominal subannual resolution. The WD2014 chronology (Sigl et al., 2015) was applied to the Dome C ice core by matching the peaks in sulfate concentration relating to volcanic eruptions with those of the WAIS Divide ice core. The 54 m of the Dome C ice core covers the period 882–2008 CE.

In addition to the Dome C ice core, other, shorter records were also studied: a 2-m snow pit dug at Dome C in 2012, sampled every 3 cm and going back to 1987 CE, as well as samples from a 30-m deep ice core drilled in 1983–1984 at the South Pole (89°59'S, 139°16'W; elevation 2,835 m; mean annual temperature  $-49^\circ\text{C}$ ; accumulation 7 cm we/year). The South Pole ice core was sampled between 17.5- and 24.7-m depths, covering the period from 1800 to 1865 CE; 101 samples were subsequently measured for their  $^{10}\text{Be}$  and sulfate concentrations.

Finally, a 3.6-m Vostok snow pit (accumulation 2.2 cm we/year; Touzeau et al., 2016) sampled every 3 cm, covering the period 1949–2008 CE, described in a previous study (Baroni et al., 2011), is presented here again and reinterpreted in the context of this study.

## 2.2. Sample Preparation and Measurements

$^{10}\text{Be}$  samples ( $\approx 100$  g) were prepared according to the procedure described in Baroni et al., 2011; Raisbeck et al., 2007 and were measured using the French Accelerator Mass Spectrometer national facility, ASTER (Arnold et al., 2010). The  $^{10}\text{Be}$  concentration was calculated from the  $^{10}\text{Be}/^9\text{Be}$  ratio provided by the Accelerator Mass Spectrometer and normalized to the National Institute of Standards and Technology 4325 Standard Reference Material ( $(2.79 \pm 0.03) 10^{-11}$ ; Nishiizumi et al., 2007) for a  $^{10}\text{Be}$  half-life of  $(1.387 \pm 0.012)$  Ma (Chmeleff et al., 2010; Korschinek et al., 2010). A commercial beryllium 9 ( $^9\text{Be}$ ) carrier ( $^{\text{TM}}$ Scharlau), having a  $^{10}\text{Be}/^9\text{Be}$  ratio of  $4.2 \times 10^{-15}$  (standard deviation (SD) =  $0.7 \times 10^{-15}$ , 130 samples), was used for the sample preparation and the processing blanks. The ice core samples showed mean  $^{10}\text{Be}/^9\text{Be}$  ratios of  $4.5 \times 10^{-13}$  (SD =  $1.3 \times 10^{-13}$ ) at Dome C,  $4.4 \times 10^{-13}$  (SD =  $1.0 \times 10^{-13}$ ) at Vostok, and  $5.2 \times 10^{-13}$  (SD =  $1.2 \times 10^{-13}$ ) at the South Pole. These ratios are above the quantification limit which corresponds to 10 times the standard deviation on processing blanks measurements (quantification limit =  $10 \times 0.7 \times 10^{-15} = 7 \times 10^{-15}$ ). The  $2\sigma$  error on counting statistics is 6.4%. The Dome C, South Pole, and Vostok sulfate concentration was measured by ion chromatography at the Institut des Géosciences de l'Environnement (Ginot et al., 2014) from a 5-g aliquot taken when the ice sample was melted and before the carrier was added.

Mean  $^{10}\text{Be}$  concentration of  $6.2 \times 10^4$  atoms per gram (at./g) (SD =  $1.5 \times 10^4$  at./g) and  $3.9 \times 10^4$  at./g (SD =  $0.8 \times 10^4$  at./g) were obtained in the ice cores of Dome C and South Pole, respectively, and values of  $5.2 \times 10^4$  at./g (SD =  $1.2 \times 10^4$  at./g) and  $7.9 \times 10^4$  at./g (SD =  $1.8 \times 10^4$  at./g), were measured in the snow pits of Dome C and Vostok, respectively.

## 3. Results and Discussion

### 3.1. Identification of Volcanic Eruptions and Their Imprint in the $^{10}\text{Be}$ Records

Under nonvolcanic conditions (i.e., background conditions), the main source of sulfate on the High Antarctic Plateau is of marine and biogenic origin (Legrand, 1995), it contributes to a background sulfate concentration determined for each site. The detection of volcanic imprints in ice cores was set above the sulfate background concentration. At Dome C this limit was determined to be 80 ng/g from 1900 CE to 2008 CE, and 130 ng/g before 1900 CE. At South Pole and Vostok, the limits were 74 and 103 ng/g, respectively. Based on this, 26 volcanic eruptions were detected and studied (Table 1 and Figures 1–7). The identification and ages of the volcanic events are based on the WAIS Divide (Antarctica) and the NEEM (Greenland) ice cores, annually dated (Sigl et al., 2013, 2015). All ages are given in CE. The nomenclature used here for unknown events (UE) is “age UE”. For example, “1809 UE”, refers to an unknown event recorded in 1809 CE.

The comparison between  $^{10}\text{Be}$  and sulfate profiles shows a near systematic concomitance between the two at the time of volcanic eruptions on all sites (Figures 1–7). Only two volcanic eruptions, in 1269 and in 1276, stand out from the others, showing a decrease in  $^{10}\text{Be}$  concentration at the time of sulfate peaks.

**Table 1**  
Volcanic Signals Studied

Eruption	Age (CE)	Site	Number of points	Maximal <sup>10</sup> Be concentration (10 <sup>4</sup> at./g)	Increase in <sup>10</sup> Be concentration (%)	Slope (α; at./ng)	Uncertainty on a (at./ng)	Intercept (b; 10 <sup>4</sup> at./g)	Uncertainty on b (10 <sup>4</sup> at./g)	R	Significance	Detection in the five VOLSOL ice cores	Nature of the eruption based on <sup>10</sup> Be	Nature of the eruption based on sulfur isotopes <sup>a</sup>	Bipolar volcanic signals <sup>b</sup>
Pinatubo	1991	DC <sup>(c)</sup>	5	7.32	18%	397	114	1.58	1.41	0.89	Y	n/a	stratospheric	stratospheric	bipolar
Pinatubo	1991	DC <sup>(sp)</sup>	8	6.9	33%	313	243	1.84	3.70	0.47	N	n/a	stratospheric	stratospheric	bipolar
Pinatubo	1991	VK <sup>a</sup>	5	10.3	31%	275	56	2.23	1.34	0.94	Y	n/a	stratospheric	stratospheric	bipolar
Agung	1963	DC	5	9.12	48%	152	79	5.29	1.39	0.74	N	n/a	stratospheric	stratospheric	bipolar
Agung	1963	VK <sup>a</sup>	6	13.3	68%	246	72	5.16	1.88	0.86	Y	n/a	stratospheric	stratospheric	bipolar
Cosiguina	1835	DC	7	6.92	12%	149	240	3.07	5.19	0.26	N	2/5	?	stratospheric	bipolar
Cosiguina	1835	PS	4	4.44	14%	166	32	1.44	0.41	0.96	Y	n/a	stratospheric	stratospheric	bipolar
Tambora	1815	DC	4	8.33	34%	67	51	4.41	2.09	0.68	N	3/5	?	stratospheric	bipolar
Tambora	1815	PS	6	5.80	49%	16	8	4.32	0.34	0.70	N	n/a	?	stratospheric	bipolar
U.E.	1809	DC	4	10.3	65%	72	10	6.20	0.45	0.98	Y	5/5	stratospheric	stratospheric	bipolar
U.E.	1809	PS	5	5.81	49%	101	57	3.50	0.85	0.72	N	n/a	?	stratospheric	bipolar
U.E.	1762	DC	3	9.06	46%	201	301	3.94	5.76	0.56	N	3/5	?	stratospheric	bipolar
U.E. (Serua ?)	1695	DC	7	9.58	54%	198	78	2.95	2.35	0.75	Y	3/5	stratospheric	stratospheric	bipolar
U.E.	1621	DC	5	9.46	53%	41	28	7.37	0.79	0.66	N	3/5	tropospheric	tropospheric	unipolar
Huaynaputina	1600	DC	7	9.35	51%	42	35	7.35	0.83	0.47	N	2/5	?	stratospheric	bipolar
Kuwa	1459	DC	7	13.1	112%	102	32	5.50	1.37	0.82	Y	5/5	stratospheric	stratospheric	bipolar
U.E. (A)	1286	DC	6	11.6	87%	150	54	5.76	1.65	0.81	Y	5/5	stratospheric	stratospheric	bipolar
U.E. (B)	1276	DC	7	9.24	49%	-76	65	8.67	2.26	0.46	N	5/5	?	stratospheric	unipolar
U.E. (C)	1269	DC	8	9.24	49%	-202	68	12.5	1.75	0.77	Y	3/5	stratospheric	tropospheric	unipolar
Samalas	1259	DC	9	9.38	51%	60	24	3.11	1.36	0.68	Y	5/5	stratospheric	stratospheric	bipolar
U.E.	1241	DC	5	8.45	36%	523	109	-4.58	2.29	0.94	Y	3/5	stratospheric	n/a	unipolar
U.E. (D)	1230	DC	5	8.66	40%	92	70	5.09	2.00	0.61	N	5/5	?	stratospheric	bipolar
U.E. (E)	1190	DC	10	8.16	32%	241	112	0.46	2.83	0.61	N	3/5	?	stratospheric	bipolar
U.E. (F)	1172	DC	8	11.1	79%	196	34	1.18	1.28	0.92	Y	5/5	stratospheric	stratospheric	bipolar
U.E.	1110	DC	4	7.78	26%	268	55	1.08	1.18	0.96	Y	4/5	stratospheric	stratospheric	bipolar
U.E.	1040	DC	6	12.4	101%	702	125	-5.05	2.49	0.94	Y	4/5	stratospheric	stratospheric	unipolar

Note. Names of volcanic events are indicated in the first column, U.E. means Unknown Events. Events named U.E. (A) to U.E. (F) correspond to the terminology used by Baroni et al. (2008). For known events, ages of the volcanic eruptions are given; for unknown events, ice ages are given. Maximal <sup>10</sup>Be concentration along the volcanic deposition is indicated, and the increase relative to the mean <sup>10</sup>Be concentration is indicated. Slopes and intercepts of the linear regression between <sup>10</sup>Be and sulfate concentration are given with their respective uncertainties given for a confidence level of 95%, as well as the corresponding correlation coefficient (R). A Fischer-Snedecor statistical test was applied to each individual volcanic event to determine the significance of the <sup>10</sup>Be/sulfate relationship at a confidence level of 95% (see section 3.1. for details). Y = Yes and N = No. Each significant event is classified as stratospheric and compared with independent methods that are (i) sulfur isotopic anomaly in sulfate (Baroni et al., 2008, 2007; Cole-Dai et al., 2009, 2013; Gauthier et al., 2019; Lanciki et al., 2019; Savarino, Romero, et al., 2003) and (ii) synchronous bipolar volcanic signals (Sigt et al., 2013, 2015); n/a stands for not available. The Pinatubo event has been recorded in both a Dome C snow pit (DC<sup>SP</sup>) and in a Dome C ice core (DC<sup>IC</sup>). As part of the VOLSOL project, six ice cores were drilled 1 m apart at Concordia/Dome C in 2010/2011; one was dedicated to the analysis of <sup>10</sup>Be (this work), and the other five to the isotopic composition of sulfate (Gauthier et al., 2016, 2018, 2019). The detection of the volcanic events on the five ice cores used for the isotopic composition of sulfate (Gauthier et al., 2016) is indicated in the column "VOLSOL"; 2/5 means that an event was detected in two of the five ice cores. The 14 volcanic events with a significant relationship between the <sup>10</sup>Be and the sulfate concentrations are highlighted in colors corresponding to the four groups of slope values (section 3.3.1; orange for Group 1, red for Group 2, gray for Group 3, and green for Group 4). <sup>a</sup>Sulfur isotopic anomaly in sulfate (Baroni et al., 2008, 2007; Cole-Dai et al., 2009, 2013; Gauthier et al., 2019; Lanciki et al., 2019; Savarino, Romero, et al., 2003). <sup>b</sup>Synchronous bipolar volcanic signals (Sigt et al., 2013, 2015).

The increase in  $^{10}\text{Be}$  concentration calculated from the average over the entire time range of each  $^{10}\text{Be}$  record vary between 31% and 112%, which corresponds to the extreme values reached during the Pinatubo and the Kuwae eruptions, respectively (Table 1). It is higher than that expected for the modulation of global (15%) and polar (22%)  $^{10}\text{Be}$  production, as modulated by the 11-year solar cycle over the last 60 years (Poluianov et al., 2016). The increase in  $^{10}\text{Be}$  concentration of only 18% from the Pinatubo eruption, as recorded in the Dome C ice core, is exceptionally low, with higher values of 33% and 31% found in the Dome C and Vostok snow pits, respectively. At Dome C, the mean  $^{10}\text{Be}$  concentration is higher in the ice core than in the snow pit; as a result, the increase, calculated relatively to it, is lower in the ice core than in the snow pit. This difference is due to the numerous solar minima of the last millennium (Dalton, Maunder, Spörer, Wolf, and Oort) which cause increases in  $^{10}\text{Be}$  production and therefore increases in mean  $^{10}\text{Be}$  concentration in the Dome C ice core, as compared with that of the Dome C snow pit, which covers only the last 20 years with no solar minimum. Only Cosiguina shows slight increases of 12% and 14% in  $^{10}\text{Be}$  concentration in Dome C and South Pole records, respectively.

The relationship between  $^{10}\text{Be}$  and sulfate concentrations was studied for each of the 26 eruptions detected in the different records to determine whether a volcanic eruption affected the  $^{10}\text{Be}$  signal and, if so, whether the eruption was stratospheric or tropospheric. A linear regression analysis was performed for each volcanic eruption. The uncertainties, given with a 95% confidence level on slopes and intercepts, are shown in Table 1. The significance of the linear regression depends on the number of points and their dispersion; it was tested with a Fisher-Snedecor test for a 95% confidence level.

A significant correlation between the  $^{10}\text{Be}$  and the sulfate concentrations was detected in 14 of the 26 volcanic signals studied (Table 1). They are as follows: the Pinatubo eruption (Dome C ice core and Vostok snow pit; 1991), the Agung eruption (Vostok; 1963), the Cosiguina event (South Pole; 1835), the 1809 UE (Dome C), the 1695 UE (or Serua), the Kuwae event (1459), the 1286 UE, the 1269 UE, the Samalas event (1257), the 1241 UE, the 1172 UE, the 1110 UE, and the 1040 UE all recorded at Dome C.

The 12 volcanic events that do not show a significant relationship between  $^{10}\text{Be}$  and sulfate concentrations are as follows: the Pinatubo (Dome C snow pit), Agung (Dome C ice core), Cosiguina (Dome C), the Tambora (Dome C and South Pole), the 1809 UE (South Pole), the 1762 UE, the 1621 UE, the Huaynaputina (1600), the 1276 UE, the 1230 UE, and the 1190 UE recorded at Dome C.

We can see that some events were studied from two sites but were found to be significant at only one site (Pinatubo, Agung, Cosiguina, and 1809 UE). Variability in sulfate concentration for the same event may exist between different sites (Gao et al., 2007; Sigl et al., 2015) and even at a single site (Gautier et al., 2016). This has been shown for the eruption of Tambora, one of the three most important volcanic eruptions of the last millennium (Toohey & Sigl, 2017), which is recorded in only three of the five ice cores drilled, 1 m apart, in 2010/2011 (Table 1) on the Dome C site (Gautier et al., 2016), such as that used for this study. Dome C is a low-accumulation site; consequently, snow drift and surface roughness explain variability in the record of volcanic events (Gautier et al., 2016) and probably the lack of correlation between the  $^{10}\text{Be}$  and the sulfate concentrations for some events. This may apply to the Pinatubo, the Agung, the Cosiguina, the Tambora, the 1762 UE, the 1621 UE, the Huaynaputina (1600), and the 1190 UE which exhibit a high variability in their record on the five ice cores of the VOLSOL project (Gautier et al., 2016; Table 1). As a consequence, the stratospheric nature of the Tambora, the 1762 UE, the Huaynaputina (1600), and the 1190 UE, inferred from the presence of a sulfur isotopic anomaly (Baroni et al., 2008; Gautier et al., 2019) and by their bipolar sulfate deposition (Sigl et al., 2013, 2015), is not seen in the  $^{10}\text{Be}$  records. The 1621 UE is only visible in Antarctica (Sigl et al., 2013, 2015) and has no sulfur isotopic anomaly suggesting it is tropospheric (Gautier et al., 2019); it might also be the reason that there is no correlation between  $^{10}\text{Be}$  and sulfate concentrations. Only the 1276 UE and the 1230 UE are recorded in the five VOLSOL ice cores but do not show a significant correlation between  $^{10}\text{Be}$  and sulfate concentrations despite their stratospheric nature (Gautier et al., 2019).

Volcanic events with a significant relationship between sulfate and  $^{10}\text{Be}$  concentrations correspond to stratospheric eruptions identified by the presence of a sulfur isotopic anomaly in the volcanic sulfate, for the following: the Pinatubo event (1991), the Agung event (1963), the Cosiguina event (1835), the 1809 UE, the 1695 UE (or Serua event), the Kuwae event (1459), the 1286 UE, the Samalas event (1257), the 1172 UE,

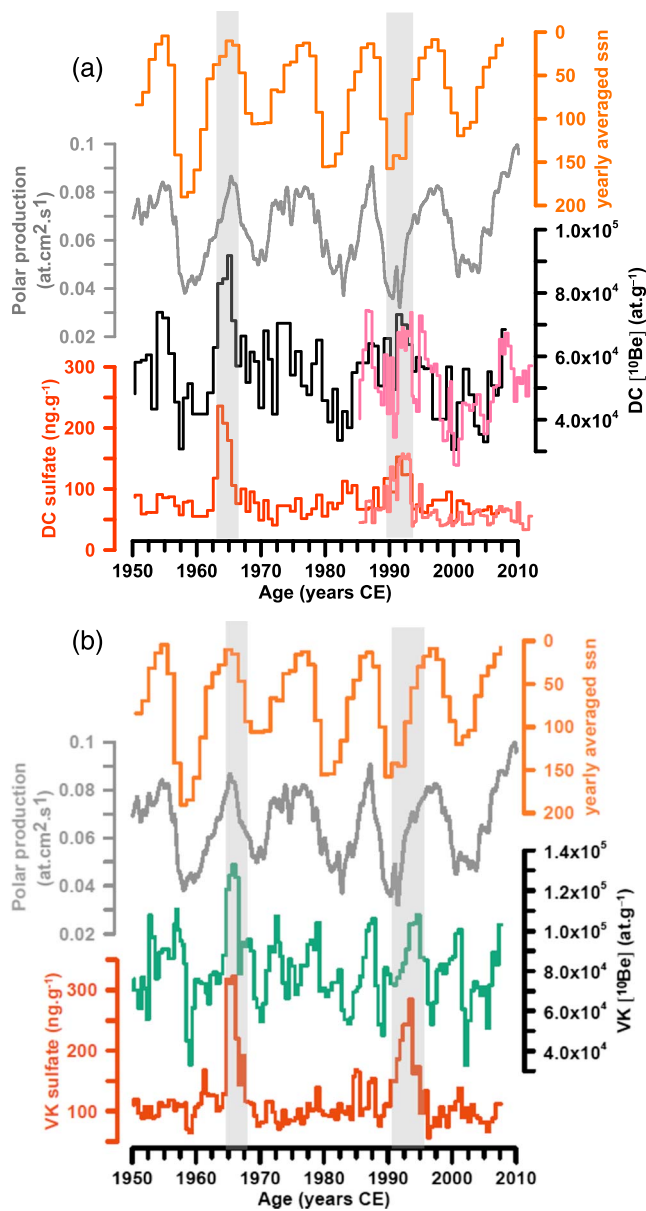


**Figure 1.** Period: 1950–2010 CE.  $^{10}\text{Be}$  and sulfate concentrations, shown as a function of time (a) at Dome C (DC) and (b) at Vostok (VK) (a)  $^{10}\text{Be}$  concentration from the Dome C ice core and from the Dome C snow pit are shown in black and pink, respectively. When available, solar proxies are represented for comparison. Polar  $^{10}\text{Be}$  production from Poluianov et al. (2016) is shown for the 1950–2010 CE period covering the neutron monitor era. Yearly averaged sunspot numbers are represented from 1950 CE to 2010 CE (<http://www.sidc.be/silso>).

the 1110 UE, and the 1040 UE (Table 1; Baroni et al., 2008, 2007; Cole-Dai et al., 2009, 2013; Gautier et al., 2019; Lanciki et al., 2012; Savarino, Romero, et al., 2003). All these volcanic events are bipolar except the 1040 UE which is detected only in Antarctica (Sigl et al., 2013, 2015).

Based on the  $^{10}\text{Be}$  record of Dome C, the 1269 UE and the 1241 UE, detected only in Antarctica (Sigl et al., 2013, 2015), are classified as stratospheric. Because of its sulfur isotopic composition, the 1269 UE has been classified as tropospheric by Gautier et al. (2019); however, among the three samples analyzed, one exhibits a  $\Delta^{33}\text{S}$  value of  $0.10 \pm 0.09\%$  which might be interpreted as a stratospheric signature. The difference between the classification of a volcanic event as tropospheric based on the sulfur isotopic anomaly of sulfate and as stratospheric based on  $^{10}\text{Be}$  records could provide information on the altitude reached by  $\text{SO}_2$  emitted by a volcano. The sulfur isotopic anomaly is expected to disappear below the ozone layer where wavelengths are longer than 310 nm, while the  $^{10}\text{Be}$  reservoir is located in the lowermost stratosphere between 10 and 15 km of altitude (Poluianov et al., 2016). Therefore, a volcanic eruption that would have reached the lowermost stratosphere would leave an imprint in  $^{10}\text{Be}$  records but no sulfur isotopic anomaly in the sulfate.

Our study provides evidences on the stratospheric nature of the 1269 UE and the 1241 UE, detected only in Antarctica (Sigl et al., 2013, 2015) and newly identified as stratospheric.

The near-systematic increase in  $^{10}\text{Be}$  concentration at the time of sulfate peaks corresponding to stratospheric eruptions, and the agreement between three different, complementary, and independent methods, show that  $^{10}\text{Be}$  can also be used as an indicator for the detection of stratospheric events.

### 3.2. Stratospheric Volcanic Eruptions and $^{10}\text{Be}$ Deposition: Mechanism

Now that the impact of stratospheric eruptions on  $^{10}\text{Be}$  deposition has been shown, the question of the mechanism arises. As proposed by Baroni et al. (2011), the underlying mechanism is the acceleration of the sedimentation of sulfate aerosols in the stratosphere, which drags  $^{10}\text{Be}$  atoms along in their path. However, this is just part of the explanation, and the reason that this volcanic imprint is so visible in  $^{10}\text{Be}$  ice core records is that (i) the  $^{10}\text{Be}$  reservoir is in the polar stratosphere at altitudes of between 10 and 15 km (Delaygue et al., 2015; Poluianov et al., 2016) and (ii) the  $^{10}\text{Be}$  snow signal is controlled by stratospheric intrusions even in nonvolcanic conditions. This last point is the keystone of the mechanism and is discussed here alongside the literature concerning  $^{10}\text{Be}$  deposition on the High Antarctic Plateau under nonvolcanic conditions. We propose here a new interpretation of existing data before extending the interpretation of the linear relationship between  $^{10}\text{Be}$  and sulfate concentrations at the time of volcanic eruptions.

As observed by in situ air measurements (Jordan et al., 2003; Raisbeck et al., 1981) and as predicted by a 2-D chemistry-transport model (Delaygue et al., 2015), the  $^{10}\text{Be}$  polar stratospheric reservoir is roughly 100 times more important than in the polar troposphere, despite an expected factor of 10 given by production models (e.g., Poluianov et al., 2016). In nonvolcanic conditions, aerosol lifetime is on the order of 1 to 2 years in the stratosphere and a few days in the troposphere. Consequently,  $^{10}\text{Be}$  atoms can accumulate and thus render the stratospheric reservoir much more important than production alone can predict (e.g., Delaygue et al., 2015).

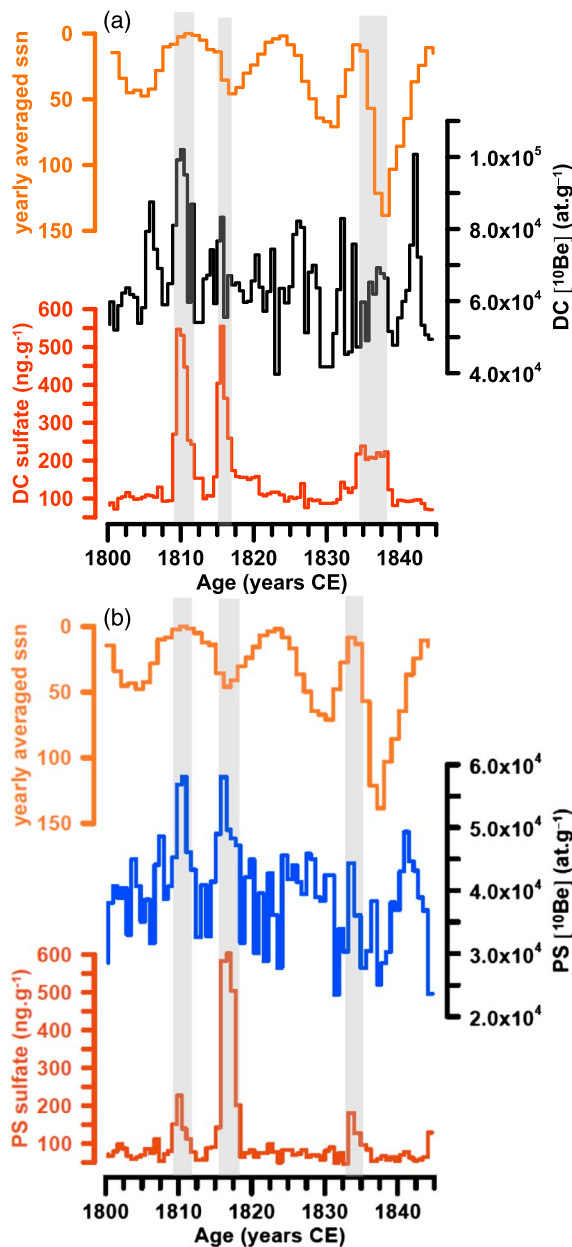


**Figure 2.** Period: 1800–1850 CE. <sup>10</sup>Be and sulfate concentrations, shown as a function of time, (a) at Dome C (DC) and (b) at South Pole (SP). When available, solar proxies are represented for comparison. Yearly averaged sunspot numbers are represented from 1800 CE to 1850 CE (<http://www.sidc.be/silso>).

Based on <sup>10</sup>Be and <sup>7</sup>Be concentrations measured in the air, in the polar stratosphere and at the South Pole station, Raisbeck et al. (1981) estimated a contribution of air from the stratosphere at 5%, but until today there has been a lack of information for the Dome C station. Recently, <sup>10</sup>Be concentration was measured in air filters collected during the year 2008 at Dome C (Legrand et al., 2017). A strong seasonality was observed in the atmospheric <sup>10</sup>Be concentration, varying from  $5 \times 10^3$  at./m<sup>3</sup> in winter to  $6.65 \times 10^4$  at./m<sup>3</sup> in summer. The <sup>10</sup>Be/<sup>7</sup>Be ratio also exhibits a seasonal variation, with values ranging from 0.6 in winter to 1.5–2 in summer. On this basis, Legrand et al. (2017) conclude that summer values are due to stratospheric intrusions at Dome C being twice as large as in winter. However, the local <sup>10</sup>Be production, which may explain the low winter <sup>10</sup>Be values, was not considered. Dome C is located at 3.2 km altitude and has an atmospheric pressure of approximately 630 hPa. The expected <sup>10</sup>Be polar production at that site would be  $5.1 \times 10^3$  at./m<sup>3</sup>.week<sup>-1</sup> (Poluianov et al., 2016), for a modulation potential of 450 MeV prevailing in July/August 2008 (Usoskin et al., 2017). This is in agreement with the values of  $5 \times 10^3$  at./m<sup>3</sup> obtained from the aerosols, collected weekly at Dome C (Legrand et al., 2017) during this period. The low <sup>10</sup>Be concentration in the winter atmosphere at Dome C may indicate a local, tropospheric <sup>10</sup>Be production. In this case, stratospheric intrusions seem to occur almost exclusively in summer.

A mixing ratio can be calculated from local tropospheric <sup>10</sup>Be production at Dome C given by the winter value of  $5 \times 10^3$  at./m<sup>3</sup> (Legrand et al., 2017) and from the <sup>10</sup>Be concentration in the low polar stratosphere when <sup>10</sup>Be atoms attached to aerosols are ready to enter the troposphere. Of the only two studies to have reported <sup>10</sup>Be concentration in the polar stratosphere (Jordan et al., 2003; Raisbeck et al., 1981), we chose that of Jordan et al. (2003) because samples were collected in October 1997 ( $3.7 \times 10^6$  at./m<sup>3</sup>), at which time the modulation potential was close to that prevailing in June/July 2008, when air samples were collected at Dome C (Legrand et al., 2017). With these two end-members, the summer <sup>10</sup>Be concentration of  $6.65 \times 10^4$  at./m<sup>3</sup> in the Dome C atmosphere would be the result of a 2% stratospheric intrusion. This value is consistent with an independent estimate of 4%, based on activity of <sup>35</sup>S (half-life = 87 days) measured from sulfate in aerosols year-round collected at Dome C, in 2010 (Hill-Falkenthal et al., 2013).

The <sup>10</sup>Be snow/ice signal at Dome C, South Pole, and probably at Vostok, all three of which are located on the High Antarctic Plateau, is controlled by a few percent of stratospheric intrusions, meaning that any change in the aerosols load in the stratosphere will be seen in <sup>10</sup>Be time series. This explains the role played on <sup>10</sup>Be deposition by volcanic aerosols formed in the stratosphere.

### 3.3. Meaning of the Slope and the Intercept

Based on the conclusions of the previous section, we will now consider the results obtained in this study to investigate the meaning of the linear correlation between the <sup>10</sup>Be and the sulfate concentrations of the 14 significant volcanic events (Table 1). Using a linear regression may seem simplistic since the processes underlying the relationship between <sup>10</sup>Be and sulfate concentrations in snow are not linear as they involve the microphysics of aerosol transport under unique volcanic eruption source parameters. Since each volcanic event is represented by five points on average, using a polynomial

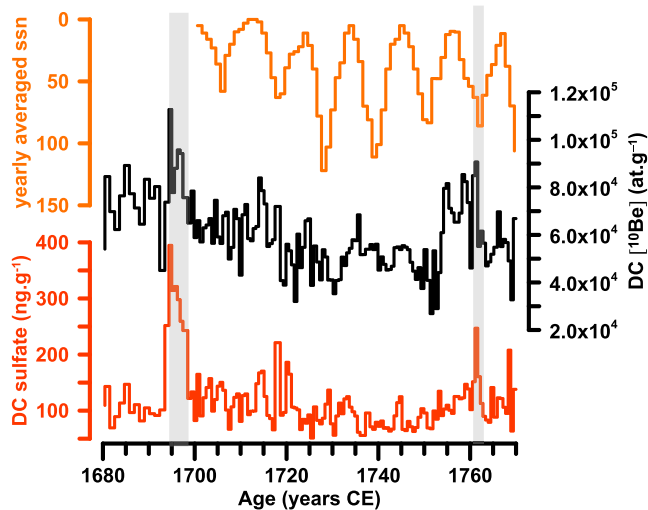


**Figure 3.** Period: 1680–1770 CE.  $^{10}\text{Be}$  and sulfate concentrations from Dome C, shown as a function of time. Yearly averaged sunspot numbers are represented from 1700 CE to 1770 CE (<http://www.sidc.be/silso>).

### 3.3.1. Slope values

It is proposed to combine hypothesis testing and clustering as used in Viseur et al. (2014). The hypothesis testing between two regression slopes of independent samples (Clogg et al., 1995; Cohen, 1983) provides the observed values of the statistic  $t_{ij}$  between slope pairs  $\hat{a}_i$  and  $\hat{a}_j$ . Then,  $t_{ij}$  is chosen as the distance metric in a hierarchical agglomerative clustering algorithm to cluster statistically similar slopes. The average link was tested as aggregation criteria in the hierarchical agglomerative clustering. Four groups of slopes have been defined; they are distributed as follows:

1. *Group 1* is made up of the highest number of volcanic events (7) which are the Pinatubo (with merged data from Dome C and Vostok), Agung, Cosiguina, Serua, 1286 UE, 1172 UE, and the 1110 UE. Slopes vary within a factor of 1.6, from  $(150 \pm 54)$  at./ng to  $(247 \pm 72)$  at./ng for the 1286 UE and Agung event, respectively (Table 1). As Pinatubo exhibits a significant correlation between the  $^{10}\text{Be}$  and sulfate concentrations at two sites, Dome C and Vostok, all the data have been merged in order to increase the total number of points (from 5 for each site to 10 for merged data). Using the  $^{10}\text{Be}$  and sulfate concentrations from merged data for Pinatubo at Dome C and Vostok, the slope is  $(219 \pm 25)$  at./ng and  $(184 \pm 36)$  at./ng

when using fluxes to take into account the slight difference in accumulation rates between both sites (2.5 cm we/year at Dome C and 2.2 cm we/year at Vostok) (Figure 8). In both cases, the slope values are consistent within uncertainties.

Considering all the volcanic events of Group 1, the mean slope is 206 at./ng (SD = 42 at./ng) when using  $^{10}\text{Be}$  and sulfate concentrations for Pinatubo or 201 at./ng (SD = 42 at./ng) when using fluxes for Pinatubo.

In this group, the Pinatubo and Agung events are known to have injected similar amounts of  $\text{SO}_2$  at similar altitudes (13 to 15 Tg of  $\text{SO}_2$  to an altitude of 25 km (Guo et al., 2004) and 6 to 12 Tg of  $\text{SO}_2$  to heights of 20 km or even 26 km (Cadle et al., 1976; Mossop, 1964; Self & Rampino, 2012), respectively. The Cosiguina event appears to be comparable to Pinatubo (Longpré et al., 2014). All the eruptions of Group 1 have one aspect in common, which is their bipolar sulfate distribution (Sigl et al., 2013, 2015).

2. *Group 2* is made up of three events (the 1809 UE and the Kuwae and Samalas eruptions), which have lower slope values than in Group 1. These values range from  $(60 \pm 24)$  at./ng to  $(102 \pm 32)$  at./ng for the Samalas and the Kuwae events, respectively (Table 1). The mean slope of Group 2 is 78 at./ng (SD = 22 at./ng).

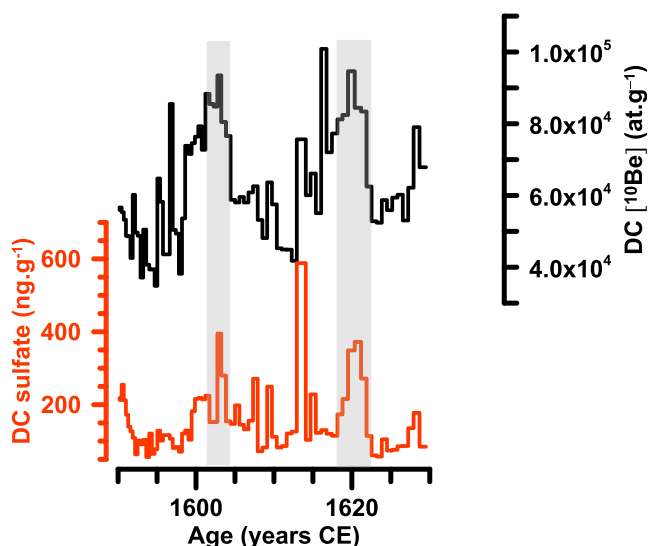


**Figure 4.** Period: 1590–1630 CE.  $^{10}\text{Be}$  and sulfate concentrations from Dome C, shown as a function of time

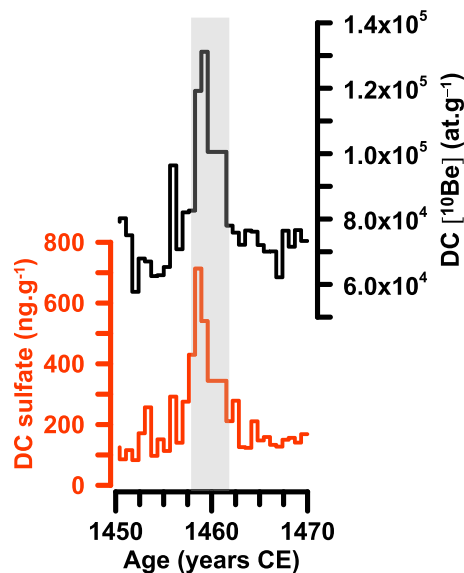


**Figure 5.** Period: 1440–1480 CE.  $^{10}\text{Be}$  and sulfate concentrations from Dome C, shown as a function of time.

These three eruptions are bipolar (Sigl et al., 2013, 2015) and are among the six largest volcanic eruptions of the last millennium (Toohey & Sigl, 2017). The Samalas eruption released  $(158 \pm 12)$  Tg of  $\text{SO}_2$  to heights of 43 km (Vidal et al., 2016), and the Kuwae event is thought to have released 100 Tg of  $\text{SO}_2$  into the atmosphere (Sigl et al., 2014). The Tambora event, the third most important, released 53–58 Tg of  $\text{SO}_2$  to 33–43 km altitude (Self et al., 2004; Sigurdsson & Carey, 1989) and has low slope values at Dome C and South Pole,  $(67 \pm 51)$  at./ng and  $(16 \pm 8)$  at./ng, respectively, which may be consistent with values of Group 2. However, the relationship between the concentrations of  $^{10}\text{Be}$  and sulfate was not significant according to the statistical test of Fisher-Snedecor (see section 3.1.) and was thus not considered.

The eruptions of Samalas, Kuwae, and Tambora released between 3 and 10 times more  $\text{SO}_2$  to altitudes at least 10 km higher than the Group 1 Pinatubo and Agung events. Group 2 appears to consist of volcanic eruptions surpassing those in Group 1 in terms of size.

3. *Group 3* comprises two events, the 1241 UE and the 1040 UE, which have the highest slopes of all the volcanic events. The mean slope of this group is 612 at./ng (SD = 127 at./ng). It is interesting to note that the 1241 UE and 1040 UE are only visible in Antarctica (Sigl et al., 2013), which suggests that the volcanoes were located in the Southern Hemisphere.
4. *Group 4.* Finally, the 1269 UE is of its own: it is the only one with a negative slope of  $(-202 \pm 68)$  at./ng. It, too, is only visible in Antarctica (Sigl et al., 2013), and this event took place 10 years after the massive volcanic eruption of Samalas.

Various trends emerge from these four groups of slope values. Slope values decrease from Group 1 to Group 2, and we know that volcanic eruptions in Group 2 released more  $\text{SO}_2$  and at higher altitudes than did those in Group 1. This suggests that slope values decrease with increasing amount of  $\text{SO}_2$  and altitude and finally with an increasing aerosol load. The Group 3 1241 UE and 1040 UE were probably located in the Southern Hemisphere inducing a proximity between the eruption site and the stratospheric polar reservoir of  $^{10}\text{Be}$ . It would have provoked an effective draining resulting in the highest slopes values among all the events studied here. In other words, it confirms that the slope would provide information on the efficiency of the draining of the  $^{10}\text{Be}$  from its stratospheric reservoir.

The Samalas event (1257) recorded in 1258–1259 in the ice and the 1269 UE occurred within a decade. They exhibit the lowest positive slope,  $(60 \pm 24)$  at./ng and the only negative slope,  $(-202 \pm 68)$  at./ng, respectively, and thus represent the extreme case of draining of the  $^{10}\text{Be}$  stratospheric reservoir. The mechanism is described below in section 3.4.

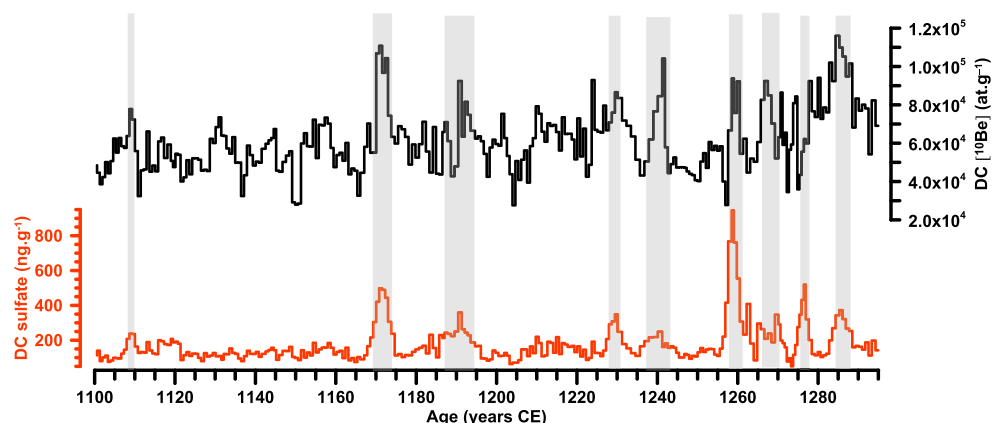


**Figure 6.** Period: 1100–1295 CE.  $^{10}\text{Be}$  and sulfate concentrations from Dome C, shown as a function of time.

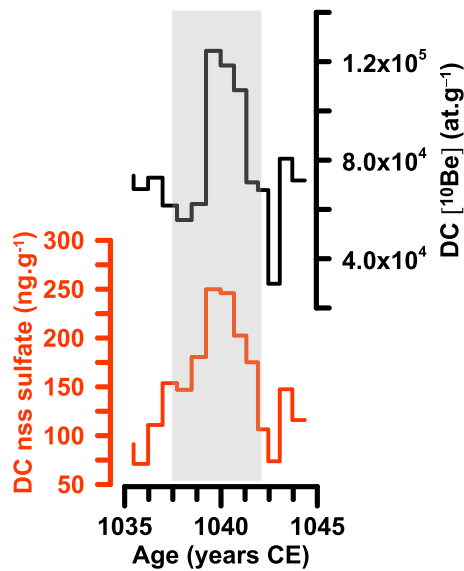


**Figure 7.** Period: 1035–1045 CE.  $^{10}\text{Be}$  and sulfate concentrations from Dome C, shown as a function of time.

at. $\text{cm}^{-3}\cdot\text{s}^{-1}$  at an altitude of between 10 and 15 km, while at the time of the Agung eruption, which occurred at a minimum of the 11-year solar cycle, the modulation coefficient was 629 MeV producing  $4.0 \times 10^{-8}$  at. $\text{cm}^{-3}\cdot\text{s}^{-1}$  (Poluianov et al., 2016; Usoskin et al., 2017). The  $^{10}\text{Be}$  polar stratospheric production between these opposite phases of the 11-year solar cycle (Figure 1) is thought to have changed by a factor of 1.7, which is in agreement with the difference between the intercepts of these two eruptions within uncertainties. This would explain, for example, why the intercept of the 1809 UE at Dome C is  $(6.20 \pm 0.45) 10^4$  at./g, which is the highest value of Groups 1 and 2 and is consistent with the low solar modulation prevailing during the Dalton Minimum (1800–1820 CE), which would have caused supplemental  $^{10}\text{Be}$  production. The increase in  $^{10}\text{Be}$  production during the Dalton Minimum is beyond the scope of this study and will not be discussed in this paper.

The intercept values of the 1241 UE and the 1040 UE are both negative; unfortunately, there is no ready explanation for this. When merging all the data points for the complete set of significant volcanic events recorded at Dome C, events which are randomly distributed over the last millennium (with the exception of the Samalas event and the 1269 UE; see section 3.4.), the intercept is  $(5.3 \pm 0.5) 10^4$  at./g (Figure 9), a value similar to the mean  $^{10}\text{Be}$  concentration of  $5.2 \times 10^4$  at./g ( $\text{SD} = 1.2 \times 10^4$  at./g) in the Dome C snow pit which covers the last 20 years. The value of intercept obtained for nine volcanic events recorded at Dome C would represent the load of the stratospheric reservoir.

### 3.4. Persistent Draining of the $^{10}\text{Be}$ Stratospheric Reservoir After the Samalas Eruption (1257 CE)

We focus on the Samalas eruption, which has the lowest positive slope ( $60 \pm 24$  at./ng) of the eruptions we study, and on the 1269 UE, which alone exhibits a negative slope ( $-202 \pm 68$  at./ng).

The lowest positive slope obtained for the Samalas eruption is thought to be the result of a long-lasting draining of  $^{10}\text{Be}$  atoms from their stratospheric polar reservoir. The slope of the 1269 UE, which occurred a decade after the Samalas event, is significantly negative ( $-202 \pm 68$  at./ng), which seems to indicate that regardless of the presence of volcanic sulfate in the stratosphere, the  $^{10}\text{Be}$  washout is not efficient because the  $^{10}\text{Be}$  reservoir is no longer in its steady state. Even if it is not significant, the 1286 UE still has a negative slope ( $-76 \pm 65$  at./ng), which means that the  $^{10}\text{Be}$  reservoir may have been impacted over 20 years after the massive Samalas event.

Even if the sulfate peak at the time of Samalas deposition is seen to persist for 3 years in the Dome C ice core before returning to background values,  $^{10}\text{Be}$  could have been washed out 10 years after. This is observed in the sulfur isotopic composition of the Samalas sulfate, with a  $\Delta^{33}\text{S}$  value of  $(-1.21 \pm 0.14)\%$ , 8 years after the

### 3.3.2. Intercepts

As the  $^{10}\text{Be}$  snow signal on the High Antarctic Plateau is controlled by the stratospheric source (section 3.2.), the intercept may provide direct information on the load of the  $^{10}\text{Be}$  stratospheric reservoir and as a result of the solar modulation at the time of the eruption for a given value of the geomagnetic field. This hypothesis can be tested on the Pinatubo and the Agung eruptions which occurred during the neutron monitor era constraining the  $^{10}\text{Be}$  production rate.

The intercepts of the Pinatubo eruption are  $(2.23 \pm 1.33) 10^4$  at./g and  $(1.58 \pm 1.41) 10^4$  at./g, at Vostok and Dome C, respectively (Table 1); for the Agung event, the values obtained at the same sites are  $(5.16 \pm 1.88) 10^4$  at./g and  $(5.29 \pm 1.39) 10^4$  at./g, respectively (Table 1). The intercept of the Pinatubo event is roughly 2 times lower than that of the Agung event. The Pinatubo eruption has one of the three lowest positive intercepts of the records, which may indicate an anomalous low  $^{10}\text{Be}$  production. This would be consistent with the modulation coefficient of 1,360–1,334 MeV prevailing in June–July 1991, at the time of the Pinatubo eruption and the highest values ever reached over the last 60 years (Usoskin et al., 2017). A modulation coefficient of 1,360 MeV would have induced a  $^{10}\text{Be}$  production of  $2.4 \times 10^{-8}$

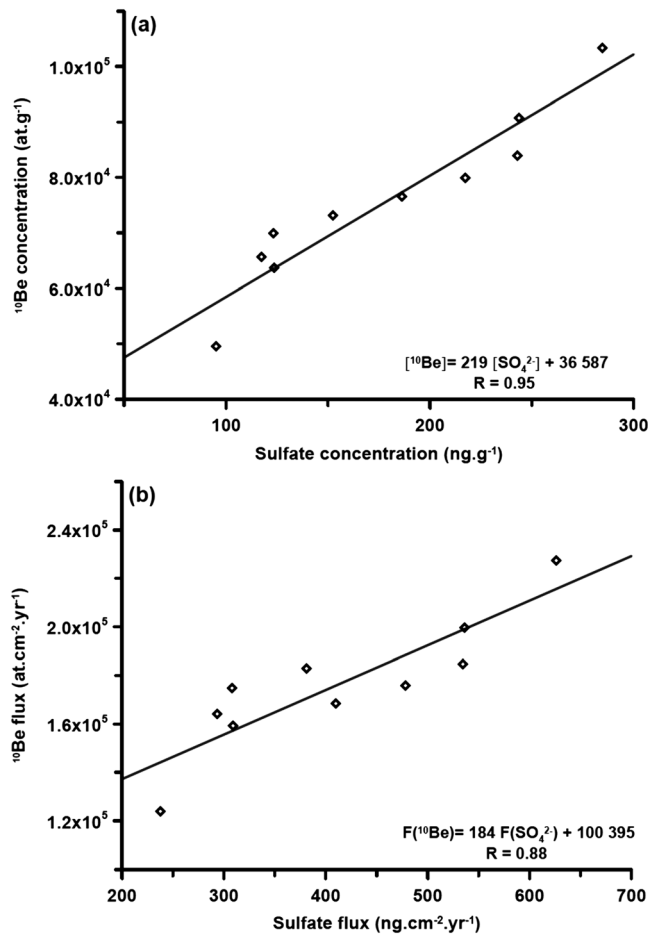


**Figure 8.** Linear regressions for Pinatubo based on merged data from Dome C and Vostok, given for (a) the  $^{10}\text{Be}$  and sulfate concentrations ( $[^{10}\text{Be}] = 219 (\pm 25)[\text{SO}_4^{2-}] + 36,587 (\pm 4,770)$ ) and (b) the  $^{10}\text{Be}$  and sulfate fluxes ( $F(^{10}\text{Be}) = 184 (\pm 36)[\text{SO}_4^{2-}] + 100,395 (\pm 15,419)$ ).

beginning of the Samalas deposition, even if the sulfate concentration is 121 ng/g almost at a background sulfate concentration set at  $(85 \pm 30)$  ng/g (supplementary material of Gautier et al., 2018; Gautier et al., 2016). This means that there were still Samalas volcanic aerosols in the stratosphere nearly a decade after the eruption, although the contribution to the sulfate snow signal became minor. This would run counter to modelling studies that predict the formation of large particle sizes and their rapid fall out, due to the large amount of  $\text{SO}_2$ , limiting the climatic impact of Samalas-type eruptions (Pinto et al., 1989; Timmreck et al., 2010, 2009). However, large amount of  $\text{SO}_2$  can also increase its lifetime and explain the persistence of an anomalous high level of sulfate aerosols in the stratosphere after the Samalas eruption. This phenomenon has been highlighted for different volcanic scenarios tested with a 2-D transport-chemistry model (Bekki, 1995; Bekki et al., 1996; Bekki & Pyle, 1994; Savarino, Bekki, et al., 2003).

Before detailing the different mechanisms that can lead to increased  $\text{SO}_2$  lifetime, it is necessary to recall that oxidation of  $\text{SO}_2$  in the stratosphere occurs in the gaseous phase by action of hydroxyl radicals (OH) according to the following reactions (Seinfeld & Pandis, 1998):



In non-volcanic conditions,  $\text{SO}_2$  lifetime is approximately 2 months (Bekki, 1995) but this can increase dramatically in volcanic conditions under influencing factors: first, a massive amount of  $\text{SO}_2$  which leads to the exhaustion of OH radicals, and second, the altitude at which the gas is injected. Both effects will delay the oxidation to sulfate and thus allow the persistence of sulfate aerosols in the stratosphere and the continuous draining of  $^{10}\text{Be}$  atoms from their reservoir, as in the case with the Samalas event.

The OH reservoir could have been exhausted if it became smaller compared with the amount of  $\text{SO}_2$ . Ozone destruction may also have restrained the formation of OH radicals (Bekki, 1995) because the absorption band of  $\text{SO}_2$  peaks at 200 nm which is a sensitive wavelength for the  $\text{O}_2$  photolysis necessary for ozone formation (Bekki, 1995) and because of the release of massive amount of halogens, such as chlorine or bromine. The Samalas eruption is thought to have injected  $(227 \pm 12)$  Tg of chlorine and  $(1.3 \pm 0.3)$  Tg of bromine into the atmosphere, multiplying preindustrial concentrations by factors of 65 and 18, respectively (Vidal et al., 2016). Even if only 2% of these halogenated gases reached the stratosphere, massive ozone destruction would have been induced (Cadoux et al., 2015), and this would have been further compounded by the blocking of  $\text{O}_2$  photolysis by the 158 Tg of  $\text{SO}_2$  released by the Samalas event.

Simulations of the (R1)–(R3) cycle for the Pinatubo eruption (i.e., 15 Tg of  $\text{SO}_2$  injected between 20.5 and 31 km altitude), and for the Samalas eruption (i.e., 320 Tg of  $\text{SO}_2$  injected at heights of between 26.5 and 38 km), show that  $\text{SO}_2$  lifetime increases to more than 4 and 24 months after these eruptions, respectively (Savarino, Bekki, et al., 2003). This compares to 2 months for nonvolcanic conditions. The results for the Samalas eruption require careful interpretation owing to the fact that halogens are not taken into account in the simulation, the amount of  $\text{SO}_2$  is overestimated (320 Tg instead of 158 Tg; Lavigne et al., 2013; Vidal et al., 2016), and the altitude of injection is underestimated (38 km instead of 43 km; Lavigne et al., 2013; Vidal et al., 2016). However, these results do show that the  $\text{SO}_2$  lifetime can increase dramatically after an eruption and that of aerosols probably was.

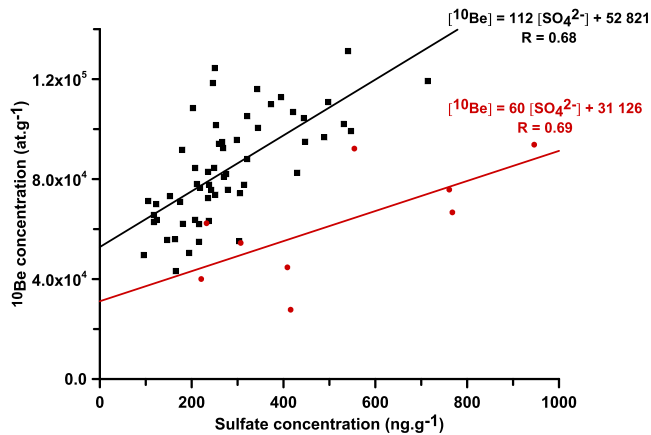


**Figure 9.**  $^{10}\text{Be}$  concentration as a function of sulfate concentration for the nine volcanic eruptions exhibiting significant correlation between these proxies (Table 1, “significance” column), for the Dome C site (black squares). The 1269 UE is not taken into account (see section 3.4.). The equation of the corresponding line is  $[^{10}\text{Be}] = 112 (\pm 16)[\text{SO}_4^{2-}] + 52,821 (\pm 4,990)$ . The red dots correspond to the Samalash volcanic eruption in 1257 CE (Lavigne et al., 2013) recorded at Dome C: the equation is  $[^{10}\text{Be}] = 60 (\pm 24)[\text{SO}_4^{2-}] + 31,126 (\pm 13,626)$  (Table 1). UE = unknown event.

Evaporation followed by photolysis of gaseous sulfuric acid back to  $\text{SO}_2$  at altitudes higher than 30 km (Delaygue et al., 2015; Rinsland et al., 1995) may also prolong the formation of sulfate aerosols. In addition, the lifetime of air masses increases to 5 years above 30 km altitude compared with 1 year for aerosols and air masses in the lower stratosphere (Delaygue et al., 2015). When this high-altitude  $\text{SO}_2$  finally returns below the limit of 30 km, it is oxidized back to sulfate and forms new sulfate aerosols, which suggests that the  $^{10}\text{Be}$  reservoir may wash out over a long time period following the end of the eruption of Samalash.

Further modelling studies are needed to distinguish the “amount” effect from the “altitude” effect, but both are also evident in the sulfur and oxygen isotopic composition of the Samalash sulfate. Samalash sulfate has the highest  $\Delta^{33}\text{S}$  values (Gautier et al., 2018; Lanciki et al., 2012) of all the volcanic events studied (Baroni et al., 2008, 2007; Cole-Dai et al., 2009, 2013; Gautier et al., 2018; Savarino, Romero, et al., 2003) and may be the result of enhanced  $\text{SO}_2$  photolysis between 34 and 43 km altitude (Whitehill et al., 2015). This  $\Delta^{33}\text{S}$  signature will be preserved once  $\text{SO}_2$  is oxidized to sulfate at lower altitudes.

The Samalash sulfate also has a near-null oxygen isotopic anomaly ( $\Delta^{17}\text{O}$ ) (Gautier et al., 2019; Savarino, Bekki, et al., 2003). Conversely to the wavelength-dependent sulfur isotopic anomaly,  $\Delta^{17}\text{O}$  is transferred by oxidative chemical species such as ozone, hydrogen peroxide, or OH radicals to sulfate (e.g., Savarino et al., 2000; Savarino & Thiemens, 1999). In the stratosphere,  $\Delta^{17}\text{O}$  of OH radicals vary between 7‰ and 30‰, from 42 to 30 km altitude, respectively (Zahn et al., 2006): of this, one fourth is transferred to sulfate through reactions (R1)–(R3) (Savarino, Bekki, et al., 2003). The Samalash event has a  $\Delta^{17}\text{O}$  of  $(0.7 \pm 0.2)\%$ , on average, which may be inherited, in part, from OH radicals at 40 km altitude (Gautier et al., 2019; Savarino, Bekki, et al., 2003), but it may also be the result of the creation of a new oxidation pathway via  $\text{O}(^3\text{P})$ , which has no oxygen isotopic anomaly, given that oxidation via OH radicals would have been exhausted by the massive injection of  $\text{SO}_2$  into the stratosphere (Savarino, Bekki, et al., 2003). Recently, another volcanic event in 426 BCE was found to display  $\Delta^{17}\text{O}$  values varying from 4‰ to 0.5‰ from the beginning to the end of the volcanic sulfate deposition, the latest values being comparable with that of Samalash (Gautier et al., 2019). The collapse of  $\Delta^{17}\text{O}$  values would be the result of sulfate formed at different altitudes and successively deposited on the ice sheet and support the “altitude effect” of Samalash-type eruptions (Gautier et al., 2019).

The Samalash eruption is unique in many respects, and  $^{10}\text{Be}$  data and the isotopic composition of sulfate show its peculiarity related to the exceptional amount of  $\text{SO}_2$  released at a high altitude in the stratosphere. The  $^{10}\text{Be}$  stratospheric reservoir was probably drained out and perturbed for a decade; as a result solar reconstructions based on  $^{10}\text{Be}$  data during this time period must be effectuated carefully.

#### 4. Conclusion

We conducted a detailed study of 26 volcanic events recorded at three different Antarctic sites in order to better understand the influence of massive amounts of stratospheric volcanic sulfate aerosols on  $^{10}\text{Be}$  deposition.

Linear relationships were determined between  $^{10}\text{Be}$  and sulfate concentrations for each individual volcanic event, of which 14 exhibit a significant relationship, thus confirming enhancement in  $^{10}\text{Be}$  deposition after stratospheric eruptions (Baroni et al., 2011).

This study has allowed to confirm the stratospheric nature of the Pinatubo event (1991), the Agung event (1963), the Cosiguina event (1835), the 1809 UE, the 1695 UE (or Serua event), the Kuwae event (1459), the 1286 UE, the Samalash event (1257), the 1172 UE, the 1110 UE, and the 1040 UE and the tropospheric nature of the 1621 UE, also deduced from the isotopic sulfur anomaly (Baroni et al., 2008, 2007; Cole-Dai

et al., 2009, 2013; Gautier et al., 2018, 2019; Lanciki et al., 2012; Savarino, Romero, et al., 2003) and bipolar volcanism (Sigl et al., 2013, 2015).

We have newly identified two unknown events as stratospheric, the 1241 UE and 1269 UE, probably located in the Southern Hemisphere as they are recorded only in Antarctica (Sigl et al., 2013, 2015). They may have had a climatic impact over the last millennium (Toohey et al., 2019).

The intercept and slope of the  $^{10}\text{Be}$ /sulfate relationship provide different and complementary information. The intercept gives information on the  $^{10}\text{Be}$  polar stratospheric reservoir that is loaded to a greater or lesser degree, depending on solar modulation at the time of the volcanic eruption. Slopes values have been classified into four groups that would relate to the diversity of volcanic source parameters, particularly the amount of  $\text{SO}_2$  emitted and the altitude it reaches in the stratosphere meaning that the slope indicates efficiency of  $^{10}\text{Be}$  washout from its reservoir.

The Samalas eruption is unlike any other in that it has the lowest positive slope among other significant events. This may be the result of persistent draining of the  $^{10}\text{Be}$  reservoir through continued aerosols formation in the stratosphere because of (i) the large amount of  $\text{SO}_2$  emitted which exhausted the oxidants responsible for the formation of sulfate and (ii) the altitude at which  $\text{SO}_2$  is emitted. This hypothesis is reinforced by the volcanic eruption recorded in the ice in 1269, which itself exhibits a negative slope among all the events studied, indicating that after the Samalas eruption, the  $^{10}\text{Be}$  stratospheric reservoir was no longer in its steady state and drained out and perturbed over a decade.  $^{10}\text{Be}$  ice core records from this period should be carefully used for solar reconstruction.

Determining the linear relationship between beryllium and sulfate concentration opens up the possibility of using slope to apply a correction of the beryllium signal in order to remove the volcanic effect. This should improve the estimation of the solar component of the  $^{10}\text{Be}$  signal in ice cores.

#### Acknowledgments

The data are available in the supporting information. This study is a contribution to the VOLSOL (ANR-09-BLAN-0003-01) and the VANISH (ANR-07-VULN-013) projects which are funded by the Agence Nationale de la Recherche (ANR). This work has also been supported by the European Research Council under the European Union's Seventh Framework Programme (FP7/2007-2013)/ERC grant agreement 306045. The fieldwork at Concordia benefited from logistical support from the French Polar Institute (IPEV) and the C2FN, with the valuable contribution of J. Savarino. The South Pole ice core was obtained during the 1983–1984 field season with the logistical support of NSF to the French project "Climatopic." We thank A. Manouvrier, M. Legrand, and G. Marec for field help. We thank S. Choy, A. Duvivier, and N. Davtian for the  $^{10}\text{Be}$  sample preparation and P. Ginot, V. Lucaire, and S. Preunkert for the ion chromatography facility at IGE. We kindly acknowledge I. Usoskin and S. Poluianov for providing their model for the cosmogenic isotopes production. The ASTER AMS national facility (CEREGE, Aix-en-Provence) is supported by the INSU/CNRS, the ANR through the "Projets thématiques d'excellence" program for the "Equipements d'excellence" ASTER-CEREGE action and IRD.

#### References

- Arnold, M., Merchel, S., Bourlès, D. L., Braucher, R., Benedetti, L., Finkel, R. C., et al. (2010). The French accelerator mass spectrometry facility ASTER: Improved performance and developments. In *Nuclear Instruments and Methods in Physics Research Section B: Beam Interactions with Materials and Atoms, 19th International Conference on Ion Beam Analysis* (Vol. 268, pp. 1954–1959). <https://doi.org/10.1016/j.nimb.2010.02.107>
- Bard, E. (1997). Nuclide production by cosmic rays during the last ice age. *Science*, *277*(5325), 532–533. <https://doi.org/10.1126/science.277.5325.532>
- Bard, E., Raisbeck, G. M., Yiou, F., & Jouzel, J. (1997). Solar modulation of cosmogenic nuclide production over the last millennium: Comparison between  $^{14}\text{C}$  and  $^{10}\text{Be}$  records. *Earth and Planetary Science Letters*, *150*(3-4), 453–462. [https://doi.org/10.1016/S0012-821X\(97\)00082-4](https://doi.org/10.1016/S0012-821X(97)00082-4)
- Baroni, M., Bard, E., Petit, J. R., Magand, O., & Bourlès, D. (2011). Volcanic and solar activity, and atmospheric circulation influences on cosmogenic  $^{10}\text{Be}$  fallout at Vostok and Concordia (Antarctica) over the last 60 years. *Geochimica et Cosmochimica Acta*, *75*(22), 7132–7145. <https://doi.org/10.1016/j.gca.2011.09.002>
- Baroni, M., Savarino, J., Cole-Dai, J., Rai, V. K., & Thiemens, M. H. (2008). Anomalous sulfur isotope compositions of volcanic sulfate over the last millenium in Antarctic ice cores. *Journal of Geophysical Research*, *113*, D20112. <https://doi.org/10.1029/2008JD010185>
- Baroni, M., Thiemens, M. H., Delmas, R. J., & Savarino, J. (2007). Mass-independent sulfur isotopic compositions in stratospheric volcanic eruptions. *Science*, *315*(5808), 84–87. <https://doi.org/10.1126/science.1131754>
- Beer, J., Blinov, A., Bonani, G., Finkel, R. C., Hofman, H. J., Lelmann, B., et al. (1990). Use of  $^{10}\text{Be}$  in polar ice to trace the 11-year cycle of solar activity. *Nature*, *347*(6289), 164–166. <https://doi.org/10.1038/347164a0>
- Beer, J., Siegenthaler, U., Bonani, G., Finkel, R. C., Oeschger, H., Suter, M., & Wolfli, W. (1988). Information on past solar activity and geomagnetism from  $^{10}\text{Be}$  in the Camp Century ice core. *Nature*, *331*(6158), 675–679. <https://doi.org/10.1038/331675a0>
- Bekki, S. (1995). Oxidation of volcanic  $\text{SO}_2$ : A sink for stratospheric OH and  $\text{H}_2\text{O}$ . *Geophysical Research Letters*, *22*(8), 913–916. <https://doi.org/10.1029/95GL00534>
- Bekki, S., & Pyle, J. A. (1992). 2-D assessment of the impact of aircraft sulphur emissions on the stratospheric sulphate aerosol layer. *Journal of Geophysical Research*, *97*(D14), 15,839–15,847. <https://doi.org/10.1029/92JD00770>
- Bekki, S., & Pyle, J. A. (1994). A two-dimensional modeling study of the volcanic eruption of Mount Pinatubo. *Journal of Geophysical Research*, *99*(D9), 18,861–18,869. <https://doi.org/10.1029/94JD00667>
- Bekki, S., Pyle, J. A., Zhong, W., Toumi, R., Haigh, J. D., & Pyle, D. M. (1996). The role of microphysical and chemical processes in prolonging the climate forcing of the Toba eruption. *Geophysical Research Letters*, *23*(19), 2669–2672. <https://doi.org/10.1029/96GL02088>
- Berggren, A.-M., Beer, J., Possnert, G., Aldahan, A., Kubik, P. W., Christl, M., et al. (2009). A 600-year annual  $^{10}\text{Be}$  record from the NGRIP ice core, Greenland. *Geophysical Research Letters*, *36*, L11801. <https://doi.org/10.1029/2009GL038004>
- Cadle, R. D., Kiang, C. S., & Louis, J. F. (1976). The global scale dispersion of the volcanic clouds from major volcanic eruptions. *Journal of Geophysical Research*, *81*(18), 3125–3132. <https://doi.org/10.1029/JC081i018p03125>
- Cadoux, A., Scaillet, B., Bekki, S., Oppenheimer, C., & Druitt, T. H. (2015). Stratospheric ozone destruction by the Bronze-Age Minoan eruption (Santorini Volcano, Greece). *Scientific Reports*, *5*, 12243. <https://doi.org/10.1038/srep12243>
- Cauquoin, A., Raisbeck, G. M., Jouzel, J., Bard, E., & ASTER Team (2014). No evidence for planetary influence on solar activity 330 000 years ago. *Astronomy & Astrophysics*, *561*, A132. <https://doi.org/10.1051/0004-6361/201322879>

- Chmeleff, J., von Blanckenburg, F., Kossert, K., & Jakob, D. (2010). Determination of the  $^{10}\text{Be}$  half-life by multicollector ICP-MS and liquid scintillation counting. *Nuclear Instruments and Methods in Physics Research Section B: Beam Interactions with Materials and Atoms*, 268(2), 192–199. <https://doi.org/10.1016/j.nimb.2009.09.012>
- Clogg, C. C., Petkova, E., & Haritou, A. (1995). Statistical methods for comparing regression coefficients between models. *American Journal of Sociology*, 100(5), 1261–1293. <https://doi.org/10.1086/230638>
- Cohen, A. (1983). Comparing regression coefficients across subsamples: A study of the statistical test. *Sociological Methods & Research*, 12(1), 77–94. <https://doi.org/10.1177/0049124183012001003>
- Cole-Dai, J., Ferris, D., Lanciki, A., Savarino, J., Baroni, M., & Thiemens, M. H. (2009). Cold decade (AD 1810–1819) caused by Tambora (1815) and another (1809) stratospheric volcanic eruption. *Geophysical Research Letters*, 36, L22703. <https://doi.org/10.1029/2009GL040882>
- Cole-Dai, J., Ferris, D. G., Lanciki, A. L., Savarino, J., Thiemens, M. H., & McConnell, J. R. (2013). Two likely stratospheric volcanic eruptions in the 1450s C.E. found in a bipolar, subannually dated 800 year ice core record. *Journal of Geophysical Research: Atmospheres*, 118, 7459–7466. <https://doi.org/10.1002/jgrd.50587>
- Delaygue, G., & Bard, E. (2011). An Antarctic view of beryllium-10 and solar activity for the past millenium. *Climate Dynamics*, 36(11-12), 2201–2218. <https://doi.org/10.1007/s00382-010-0795-1>
- Delaygue, G., Bekki, S., & Bard, E. (2015). Modelling the stratospheric budget of beryllium isotopes. *Tellus B*, 67(1). <https://doi.org/10.3402/tellusb.v67.28582>
- EPICA community members (2004). Eight glacial cycles from an Antarctic ice core. *Nature*, 429(6992), 623–628. <https://doi.org/10.1038/nature02599>
- Farquhar, J., Savarino, J., Airieau, S., & Thiemens, M. H. (2001). Observation of wavelength-sensitive mass-independent sulfur isotope effects during  $\text{SO}_2$  photolysis: Implications for the early atmosphere. *Journal of Geophysical Research*, 106(E12), 32,829–32,839. <https://doi.org/10.1029/2000JE001437>
- Finkel, R. C., & Nishiizumi, K. (1997). Beryllium 10 concentrations in the Greenland Ice Sheet Project 2 ice core from 3–40 ka. *Journal of Geophysical Research*, 102(C12), 26,699–26,706. <https://doi.org/10.1029/97JC01282>
- Gao, C., Oman, L., Robock, A., & Stenchikov, G. (2007). Atmospheric volcanic loading derived from bipolar ice cores: Accounting for the spatial distribution of volcanic deposition. *Journal of Geophysical Research*, 112, D09109. <https://doi.org/10.1029/2006JD007461>
- Gautier, E., Savarino, J., Erbland, J., & Farquhar, J. (2018).  $\text{SO}_2$  oxidation kinetics leave a consistent isotopic imprint on volcanic ice core sulfate. *Journal of Geophysical Research: Atmospheres*, 123, 9801–9812. <https://doi.org/10.1029/2018JD028456>
- Gautier, E., Savarino, J., Erbland, J., Lanciki, A., & Possenti, P. (2016). Variability of sulfate signal in ice core records based on five replicate cores. *Climate of the Past*, 12(1), 103–113. <https://doi.org/10.5194/cp-12-103-2016>
- Gautier, E., Savarino, J., Hoek, J., Erbland, J., Caillon, N., Hattori, S., et al. (2019). 2600-years of stratospheric volcanism through sulfate isotopes. *Nature Communications*, 10(1), 466. <https://doi.org/10.1038/s41467-019-08357-0>
- Genot, P., Dumont, M., Lim, S., Patris, N., Taupin, J.-D., Wagnon, P., et al. (2014). A 10 year record of black carbon and dust from a Mera Peak ice core (Nepal): Variability and potential impact on melting of Himalayan glaciers. *The Cryosphere*, 8(4), 1479–1496. <https://doi.org/10.5194/tc-8-1479-2014>
- Guo, S., Rose, W. I., Bluth, G. J. S., & Watson, I. M. (2004). Particles in the great Pinatubo volcanic cloud of June 1991: The role of ice. *Geochemistry, Geophysics, Geosystems*, 5, Q05003. <https://doi.org/10.1029/2003GC000655>
- Hawkins, D. M. (2004). The problem of overfitting. *Journal of Chemical Information and Computer Sciences*, 44(1), 1–12. <https://doi.org/10.1021/ci0342472>
- Heikkilä, U., Beer, J., Abreu, J. A., & Steinhilber, F. (2013). On the atmospheric transport and deposition of the cosmogenic radionuclides ( $^{10}\text{Be}$ ): A review. *Space Science Reviews*, 176(1-4), 321–332. <https://doi.org/10.1007/s11214-011-9838-0>
- Hill-Falkenthal, J., Priyadarshi, A., Savarino, J., & Thiemens, M. (2013). Seasonal variations in  $^{35}\text{S}$  and  $\Delta^{17}\text{O}$  of sulfate aerosols on the Antarctic plateau:  $^{35}\text{S}$  and  $\Delta^{17}\text{O}$  measurements at Dome C. *Journal of Geophysical Research: Atmospheres*, 118, 9444–9455. <https://doi.org/10.1002/jgrd.50716>
- Horiuchi, K., Uchida, T., Sakamoto, Y., Ohta, A., Matsuzaki, H., Shibata, Y., & Motoyama, H. (2008). Ice core record of  $^{10}\text{Be}$  over the past millennium from Dome Fuji, Antarctica: A new proxy record of past solar activity and a powerful tool for stratigraphic dating. *Quaternary Geochronology*, 3(3), 253–261. <https://doi.org/10.1016/j.quageo.2008.01.003>
- Jordan, C. E., Dibb, J. E., & Finkel, R. C. (2003).  $^{10}\text{Be}/^7\text{Be}$  tracer of atmospheric transport and stratosphere-troposphere exchange. *Journal of Geophysical Research*, 108(D8), 4234. <https://doi.org/10.1029/2002JD002395>
- Korschinek, G., Bergmaier, A., Faestermann, T., Gerstmann, U. C., Knie, K., Rugel, G., et al. (2010). A new value for the half-life of  $^{10}\text{Be}$  by heavy-ion elastic recoil detection and liquid scintillation counting. *Nuclear Instruments and Methods in Physics Research Section B: Beam Interactions with Materials and Atoms*, 268(2), 187–191. <https://doi.org/10.1016/j.nimb.2009.09.020>
- Kovaltsov, G. A., & Usoskin, I. G. (2010). A new 3D numerical model of cosmogenic nuclide  $^{10}\text{Be}$  production in the atmosphere. *Earth and Planetary Science Letters*, 291(1-4), 182–188. <https://doi.org/10.1016/j.epsl.2010.01.011>
- Lanciki, A., Cole-Dai, J., Thiemens, M. H., & Savarino, J. (2012). Sulfur isotope evidence of little or no stratospheric impact by the 1783 Laki volcanic eruption. *Geophysical Research Letters*, 39, L01806. <https://doi.org/10.1029/2011GL050075>
- Langway, J. C. C., Osada, K., Clausen, H. B., Hammer, C. U., & Shoji, H. (1995). A 10-century comparison of prominent bipolar volcanic events in ice cores. *Journal of Geophysical Research*, 100(D8), 16,241–16,247. <https://doi.org/10.1029/95JD01175>
- Lavigne, F., Degeai, J.-P., Komorowski, J.-C., Guillet, S., Robert, V., Lahitte, P., et al. (2013). Source of the great A.D. 1257 mystery eruption unveiled, Samalas volcano, Rinjani Volcanic Complex, Indonesia. *Proceedings of the National Academy of Sciences*, 110(42), 16,742–16,747. <https://doi.org/10.1073/pnas.1307520110>
- Legrand, M. (1995). *Sulphur-derived species in polar ice: A review*, NATO ASI Series, (Vol. 130, pp. 91–119).
- Legrand, M., Preunkert, S., Weller, R., Zipf, L., Elsässer, C., Merchel, S., et al. (2017). Year-round record of bulk and size-segregated aerosol composition in central Antarctica (Concordia site)—Part 2: Biogenic sulfur (sulfate and methanesulfonate) aerosol. *Atmospheric Chemistry and Physics*, 17(22), 14,055–14,073. <https://doi.org/10.5194/acp-17-14055-2017>
- Longpré, M.-A., Stix, J., Burkert, C., Hansteen, T., & Kutterolf, S. (2014). Sulfur budget and global climate impact of the A.D. 1835 eruption of Cosigüina volcano, Nicaragua. *Geophysical Research Letters*, 41, 6667–6675. <https://doi.org/10.1002/2014GL061205>
- McCormick, M. P., Thomason, L. W., & Trepte, C. R. (1995). Atmospheric effects of the Mt Pinatubo eruption. *Nature*, 373, 399–404.
- Mekhaldi, F., Muscheler, R., Adolphi, F., Aldahan, A., Beer, J., McConnell, J. R., et al. (2015). Multiradionuclide evidence for the solar origin of the cosmic-ray events of AD 774/5 and 993/4. *Nature Communications*, 6(1), 8611. <https://doi.org/10.1038/ncomms9611>

- Miyake, F., Suzuki, A., Masuda, K., Horiuchi, K., Motoyama, H., Matsuzaki, H., et al. (2015). Cosmic ray event of A.D. 774–775 shown in quasi-annual  $^{10}\text{Be}$  data from the Antarctic Dome Fuji ice core. *Geophysical Research Letters*, *42*, 84–89. <https://doi.org/10.1002/2014GL062218>
- Mossop, S. C. (1964). Volcanic dust collected at an altitude of 20 km. *Nature*, *203*(4947), 824–827. <https://doi.org/10.1038/203824a0>
- Nishiizumi, K., Imamura, M., Caffee, M. W., Southon, J. R., Finkel, R. C., & McAninch, J. (2007). Absolute calibration of  $^{10}\text{Be}$  AMS standards. *Nuclear Instruments and Methods in Physics Research B*, *258*(2), 403–413. <https://doi.org/10.1016/j.nimb.2007.01.297>
- Ono, S., Whitehill, A. R., & Lyons, J. R. (2013). Contribution of isotopologue self-shielding to sulfur mass-independent fractionation during sulfur dioxide photolysis. *Journal of Geophysical Research: Atmospheres*, *118*, 2444–2454. <https://doi.org/10.1002/jgrd.50183>
- Pinto, J. P., Turco, R. P., & Toon, O. B. (1989). Self-limiting physical and chemical effects in volcanic eruption clouds. *Journal of Geophysical Research*, *94*(D8), 11,165–11,174. <https://doi.org/10.1029/JD094iD08p11165>
- Polunianov, S. V., Kovaltsov, G. A., Mishev, A. L., & Usoskin, I. G. (2016). Production of cosmogenic isotopes  $^7\text{Be}$ ,  $^{10}\text{Be}$ ,  $^{14}\text{C}$ ,  $^{22}\text{Na}$ , and  $^{36}\text{Cl}$  in the atmosphere: Altitudinal profiles of yield functions. *Journal of Geophysical Research: Atmospheres*, *121*, 8125–8136. <https://doi.org/10.1002/2016JD025034>
- Raisbeck, G. M., Cauquoin, A., Jouzel, J., Landais, A., Petit, J.-R., Lipenkov, V. Y., et al. (2017). An improved north–south synchronization of ice core records around the 41 kyr  $^{10}\text{Be}$  peak. *Climate of the Past*, *13*(3), 217–229. <https://doi.org/10.5194/cp-13-217-2017>
- Raisbeck, G. M., Yiou, F., Cattani, O., & Jouzel, J. (2006).  $^{10}\text{Be}$  evidence for the Matuyama-Brunhes geomagnetic reversal in the EPICA Dome C ice core. *Nature*, *444*(7115), 82–84. <https://doi.org/10.1038/nature05266>
- Raisbeck, G. M., Yiou, F., FrunEAU, M., Loiseaux, J. M., Lieuvain, M., & Ravel, J. C. (1981). Cosmogenic  $^{10}\text{Be}/^7\text{Be}$  as a probe of atmospheric transport processes. *Geophysical Research Letters*, *8*(9), 1015–1018. <https://doi.org/10.1029/GL008i009p1015>
- Raisbeck, G. M., Yiou, F., Jouzel, J., & Petit, J. R. (1990).  $^{10}\text{Be}$  and  $^2\text{H}$  in polar ice cores as a probe of the solar variability's influence on climate. *Philosophical Transactions. Royal Society of London, A300*(1615), 463–470. <https://doi.org/10.1098/rsta.1990.0027>
- Raisbeck, G. M., Yiou, F., Jouzel, J., & Stocker, T. F. (2007). Direct north-south synchronization of abrupt climate change record in ice cores using beryllium 10. *Climate of the Past*, *3*(3), 541–547. <https://doi.org/10.5194/cp-3-541-2007>
- Rinsland, C. P., Gunson, M. R., Ko, M. K. W., Weisenstein, D. W., Zander, R., Abrams, M. C., et al. (1995).  $\text{H}_2\text{SO}_4$  photolysis: A source of sulfur dioxide in the upper stratosphere. *Geophysical Research Letters*, *22*(9), 1109–1112. <https://doi.org/10.1029/95GL00917>
- Savarino, J., Bekki, S., Cole-Dai, J., & Thiemens, M. H. (2003). Evidence from sulfate mass independent oxygen isotopic compositions of dramatic changes in atmospheric oxidation following massive volcanic eruptions. *Journal of Geophysical Research*, *108*(D21), 4671. <https://doi.org/10.1029/2003JD003737>
- Savarino, J., Lee, C. C. W., & Thiemens, M. H. (2000). Laboratory oxygen isotopic study of sulfur (IV) oxidation: Origin of the mass-independent oxygen isotopic anomaly in atmospheric sulfates and sulfate mineral deposits on Earth. *Journal of Geophysical Research*, *105*(D23), 29,079–29,088. <https://doi.org/10.1029/2000JD900456>
- Savarino, J., Romero, A., Cole-Dai, J., Bekki, S., & Thiemens, M. H. (2003). UV induced mass-independent sulfur isotope fractionation in stratospheric volcanic sulfate. *Geophysical Research Letters*, *30*(21), 2131. <https://doi.org/10.1029/2003GL018134>
- Savarino, J., & Thiemens, M. H. (1999). Analytical procedure to determine both  $\delta^{18}\text{O}$  and  $\delta^{17}\text{O}$  of  $\text{H}_2\text{O}_2$  in natural water and first measurements. *Atmospheric Environment*, *33*(22), 3683–3690. [https://doi.org/10.1016/S1352-2310\(99\)00122-3](https://doi.org/10.1016/S1352-2310(99)00122-3)
- Seinfeld, J. H., & Pandis, S. N. (1998). *Atmospheric chemistry and physics*. New York: Wiley-Interscience publication.
- Self, S., Gertisser, R., Thordarson, T., Rampino, M. R., & Wolff, J. A. (2004). Magma volume, volatile emissions, and stratospheric aerosols from the 1815 eruption of Tambora. *Geophysical Research Letters*, *31*, L20608. <https://doi.org/10.1029/2004GL020925>
- Self, S., & Rampino, M. R. (2012). The 1963–1964 eruption of Agung volcano (Bali, Indonesia). *Bulletin of Volcanology*, *74*(6), 1521–1536. <https://doi.org/10.1007/s00445-012-0615-z>
- Sigl, M., McConnell, J. R., Layman, L., Maselli, O., McGwire, K., Pasteris, D., et al. (2013). A new bipolar ice core record of volcanism from WAIS Divide and NEM and implications for climate forcing of the last 2000 years. *Journal of Geophysical Research: Atmospheres*, *118*, 1151–1169. <https://doi.org/10.1029/2012JD018603>
- Sigl, M., McConnell, J. R., Toohey, M., Curran, M., Das, S. B., Edwards, R., et al. (2014). Insights from Antarctica on volcanic forcing during the Common Era. *Nature Climate Change*, *4*(8), 693–697. <https://doi.org/10.1038/nclimate2293>
- Sigl, M., Winstrup, M., McConnell, J. R., Welten, K. C., Plunkett, G., Ludlow, F., et al. (2015). Timing and climate forcing of volcanic eruptions for the past 2,500 years. *Nature*, *523*(7562), 543–549. <https://doi.org/10.1038/nature14565>
- Sigurdsson, H., & Carey, S. (1989). Plinian and co-ignimbrite tephra fall from the 1815 eruption of Tambora volcano. *Bulletin of Volcanology*, *51*(4), 243–270. <https://doi.org/10.1007/BF01073515>
- Steinhilber, F., Abreu, J. A., Beer, J., Brunner, I., Christl, M., Fischer, H., et al. (2012). 9,400 years of cosmic radiation and solar activity from ice cores and tree rings. *Proceedings of the National Academy of Sciences*, *109*(16), 5967–5971. <https://doi.org/10.1073/pnas.1118965109>
- Timmreck, C. (2012). Modeling the climatic effects of large explosive volcanic eruptions. *Wiley Interdisciplinary Reviews: Climate Change*, *3*(6), 545–564. <https://doi.org/10.1002/wcc.192>
- Timmreck, C., Graf, H.-F., Lorenz, S. J., Niemeier, U., Zanchettin, D., Matei, D., et al. (2010). Aerosol size confines climate response to volcanic super-eruptions. *Geophysical Research Letters*, *37*, L24705. <https://doi.org/10.1029/2010GL045464>
- Timmreck, C., Lorenz, S. J., Crowley, T. J., Kinne, S., Raddatz, T., Thomas, M. A., & Jungclaus, J. H. (2009). Limited temperature response to the very large AD 1258 volcanic eruption. *Geophysical Research Letters*, *36*, L21708. <https://doi.org/10.1029/2009GL040083>
- Toohey, M., Krüger, K., Schmidt, H., Timmreck, C., Sigl, M., Stoffel, M., & Wilson, R. (2019). Disproportionately strong climate forcing from extratropical explosive volcanic eruptions. *Nature Geoscience*, *12*(2), 100–107. <https://doi.org/10.1038/s41561-018-0286-2>
- Toohey, M., & Sigl, M. (2017). Volcanic stratospheric sulfur injections and aerosol optical depth from 500 BCE to 1900 CE. *Earth System Science Data*, *9*(2), 809–831. <https://doi.org/10.5194/essd-9-809-2017>
- Touzeau, A., Landais, A., Stenni, B., Uemura, R., Fukui, K., Fujita, S., et al. (2016). Acquisition of isotopic composition for surface snow in East Antarctica and the links to climatic parameters. *The Cryosphere*, *10*(2), 837–852. <https://doi.org/10.5194/tc-10-837-2016>
- Usoskin, I. G., Gil, A., Kovaltsov, G. A., Mishev, A. L., & Mikhailov, V. V. (2017). Heliospheric modulation of cosmic rays during the neutron monitor era: Calibration using PAMELA data for 2006–2010. *Journal of Geophysical Research: Space Physics*, *122*, 3875–3887. <https://doi.org/10.1002/2016JA023819>
- Vidal, C. M., Métrich, N., Komorowski, J.-C., Pratomo, I., Michel, A., Kartadinata, N., et al. (2016). The 1257 Samalas eruption (Lombok, Indonesia): The single greatest stratospheric gas release of the Common Era. *Scientific Reports*, *6*, 34868. <https://doi.org/10.1038/srep34868>
- Visser, S., Châtelée, S., Lamarche, J., 2014. Estimation of fracture density by coupling regression and hypothesis testing, in: 34th Gocad Meeting. Nancy.

- Whitehill, A. R., Jiang, B., Guo, H., & Ono, S. (2015). SO<sub>2</sub> photolysis as a source for sulfur mass-independent isotope signatures in stratospheric aerosols. *Atmospheric Chemistry and Physics*, *15*(4), 1843–1864. <https://doi.org/10.5194/acp-15-1843-2015>
- Wu, C. J., Usoskin, I., Krivova, N., Kovaltsov, G. A., Baroni, M., Bard, E., & Solanki, S. K. (2018). Solar activity over nine millennia: A consistent multi-proxy reconstruction. *Astronomy & Astrophysics*, *615*, A93. <https://doi.org/10.1051/0004-6361/201731892>
- Yalcin, K., Wake, C. P., Kreutz, K. J., Germani, M. S., & Whitlow, S. I. (2006). Ice core evidence for a second volcanic eruption around 1809 in the Northern Hemisphere. *Geophysical Research Letters*, *33*, L14706. <https://doi.org/10.1029/2006GL026013>
- Yiou, F., Raisbeck, G. M., Baumgartner, S., Beer, J., Hammer, C. U., Johnsen, S., et al. (1997). Beryllium 10 in the Greenland Ice Core Project ice core at Summit, Greenland. *Journal of Geophysical Research*, *102*(C12), 26,783–26,794. <https://doi.org/10.1029/97JC01265>
- Zahn, A., Franz, P., Bechtel, C., Groob, J.-U., & Rockmann, T. (2006). Modelling the budget of middle atmospheric water vapour isotopes. *Atmospheric Chemistry and Physics*, *6*(8), 2073–2090. <https://doi.org/10.5194/acp-6-2073-2006>